

## Corrosion Resistance of Two Ternary $\text{Mg}_{88}\text{Ti}_5\text{Si}_7$ and $\text{Mg}_{60}\text{Ti}_{10}\text{Si}_{30}$ Alloys Synthesised by Mechanical Alloying

L.Dias<sup>1</sup>, B. Trindade<sup>1\*</sup>, R. Fischer<sup>2</sup>, S. Mies<sup>2</sup>, C.M.A. Brett<sup>2</sup>

<sup>1</sup> ICEMS, Dep. de Engenharia Mecânica, Universidade de Coimbra, 3030-201 Coimbra, Portugal

<sup>2</sup> ICEMS, Dep. Química, Universidade de Coimbra, 3004-535 Coimbra, Portugal

**Keywords:** Magnesium alloys, mechanical alloying, corrosion, microstructure.

**Abstract.** The corrosion resistance of ternary  $\text{Mg}_{88}\text{Ti}_5\text{Si}_7$  and  $\text{Mg}_{60}\text{Ti}_{10}\text{Si}_{30}$  samples made by mechanical alloying, with and without heat treatment, has been investigated by the electrochemical techniques of open circuit potential, polarisation curves and electrochemical impedance. Samples were made with different milling times and were subjected to annealing at increasing temperatures. The experimental results demonstrate that corrosion is up to one order of magnitude higher for  $\text{Mg}_{88}\text{Ti}_5\text{Si}_7$  than for  $\text{Mg}_{60}\text{Ti}_{10}\text{Si}_{30}$  which is explained in terms of changes in the alloy microstructure occurring during milling and after heat treatment.

### Introduction

Magnesium alloys are expected to be used in the synthesis of light-weight components and to improve their functionality per unit weight. However, use of magnesium has been limited, especially in aerospace applications, because of its poor corrosion resistance. Titanium is one of the candidates as alloying element with magnesium since it forms a self-healing corrosion layer [1]. However, Mg and Ti are almost mutually insoluble and only far-from-equilibrium processes such as mechanical alloying (MA) and physical vapour deposition (PVD) techniques can be successfully utilised to produce these alloys. Incorporation of a third element with a great affinity for Ti and Mg might increase alloy strength by formation of fine-dispersion precipitates of intermetallic phases in the Mg matrix, giving rise to metal matrix composite (MMC) materials. This can be achieved by silicon, since it forms intermetallic compounds with Mg and Ti [2].

This paper deals with the influence of the microstructure on the corrosion behaviour of mechanically alloyed  $\text{Mg}_{88}\text{Ti}_5\text{Si}_7$  and  $\text{Mg}_{60}\text{Ti}_{10}\text{Si}_{30}$  samples with and without subsequent annealing. Milling was performed in a planetary mill. The mixtures were characterised by X-ray diffraction (XRD) and scanning electron microscopy (SEM). Differential scanning calorimetry (DSC) was used to evaluate the thermal stability of the samples.

### Experimental

Samples with nominal compositions of  $\text{Mg}_{88}\text{Ti}_4\text{Si}_7$  and  $\text{Mg}_{60}\text{Ti}_{10}\text{Si}_{30}$  were synthesised by mechanical alloying from Mg, Si and Ti powders with a nominal purity of 99.6%, 99.5% and 99.0% and average particle sizes of 60, 10 and 75  $\mu\text{m}$ , respectively. Milling was performed in a planetary ball mill using hardened steel vial (250 ml) and balls (15 balls with 20 mm diameter each). A ball-to-powder weight ratio of 20:1 was used. The rotation speed was 500 rpm. In order to avoid contamination milling was performed in an argon atmosphere. XRD, SEM and DSC were used for the powder analysis. The X-ray diffraction patterns were obtained using  $\text{Co K}_\alpha$  radiation. The heating rate of the DSC runs was  $40^\circ\text{C min}^{-1}$ . Based on the DSC curves the as-milled samples were annealed in a vacuum furnace at 300 and  $500^\circ\text{C}$  (sample  $\text{Mg}_{88}\text{Ti}_5\text{Si}_7$ ) and 500 and  $900^\circ\text{C}$  (sample  $\text{Mg}_{60}\text{Ti}_{10}\text{Si}_{30}$ ). After each annealing the structure of the mixtures was evaluated at room temperature by XRD. The mixtures were compacted into disks with 10mm diameter and 1mm thickness for the corrosion tests. These were carried out in 0.01 M NaCl and 0.1 M  $\text{Na}_2\text{SO}_4$  aqueous solutions, after mounting the samples as electrodes, in order to permit comparisons with results in the literature for

\* Corresponding author: [bruno.trindade@dem.uc.pt](mailto:bruno.trindade@dem.uc.pt)  
Licensed to Universidade de Coimbra - Polo II - Coimbra - Portugal

other magnesium alloys, e.g. [3]. Measurements of the open circuit potential and its variation with time, and the recording of polarisation curves were carried out using a Princeton Applied Research PAR 273A potentiostat, with a platinum foil auxiliary electrode and a saturated calomel electrode (SCE) as reference. Electrochemical impedance spectra were recorded with a Solartron 1250 Frequency Response Analyser coupled to a 1286 Electrochemical Interface controlled by Zplot software over the frequency range 65 kHz to 0.1 Hz using a 10 mV rms sinusoidal voltage perturbation.

## Results and Discussion

**Structural results.** Fig. 1 illustrates the structural evolution of the mixtures with milling time. In both samples, the line reflections of magnesium (major phase) gradually broaden with milling time, signifying a decrease in the structural order of this phase during the milling process. In the case of samples with 7 at.% Si, there is the formation of the intermetallic  $Mg_2Si$  from the beginning of the process (traces of this phase can be already detected in the X-ray diffraction pattern obtained after 1h of milling). The final structure of the sample with the lower silicon content is a dispersion of  $Mg_2Si$  in a Mg matrix. Concerning the  $Mg_{60}Ti_{10}Si_{30}$  sample, there is firstly the formation of  $Mg_2Si$  and later the appearance of  $Ti_5Si_3$ , consuming the whole remaining silicon.

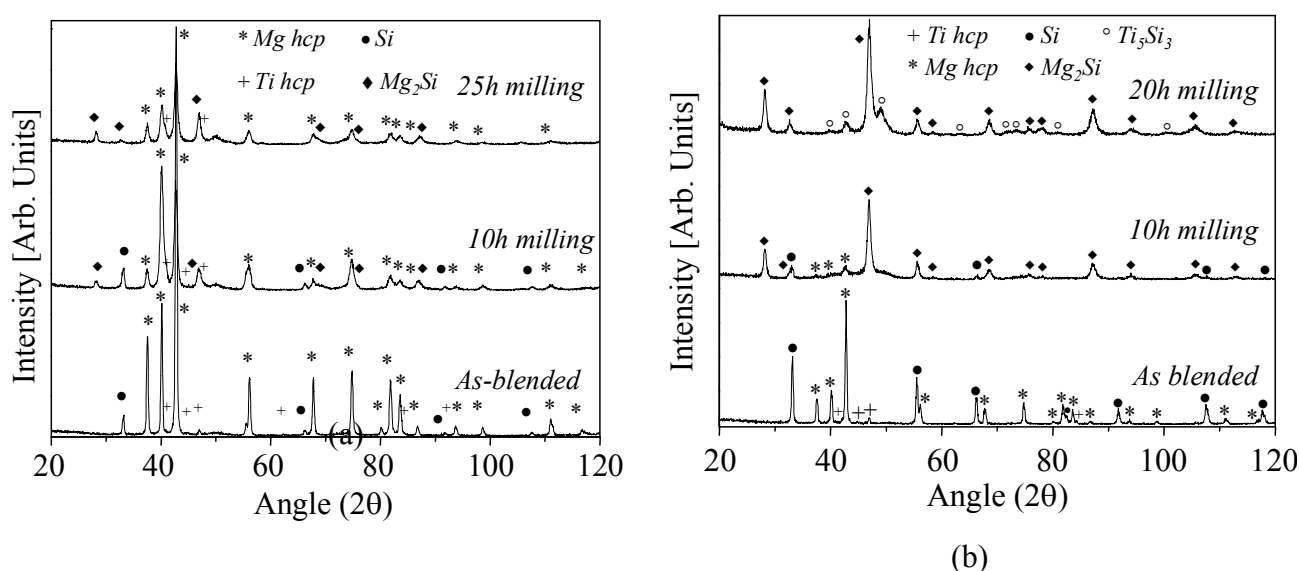


Fig. 1. Structural evolution of the (a)  $Mg_{88}Ti_5Si_7$  and (b)  $Mg_{60}Ti_{10}Si_{30}$  mixtures with milling time.

The structural results of the annealed alloys are presented in Fig.2.

The X-ray analysis performed on  $Mg_{88}Ti_5Si_7$  alloy shows very little change between the diffraction patterns of the sample before and after annealing at 300 and 500°C. The only feature to notice is the increase in peak intensities of the  $Mg_2Si$  phase and a decrease of its full width at half height (grain size increasing).

Concerning the  $Mg_{60}Ti_{10}Si_{30}$  sample, its structure after annealing at 500°C is formed by the same phases as the 20h milled sample, i.e.  $Mg_2Si$  +  $Ti_5Si_3$ . However, the XRD diffraction peaks of  $Ti_5Si_3$  situated at low diffraction angles are well defined after annealing meaning that there is a higher content of this phase in the heat-treated structure. Annealing at higher temperatures (900°C) gives rise to another intermetallic ( $TiSi_2$ ).

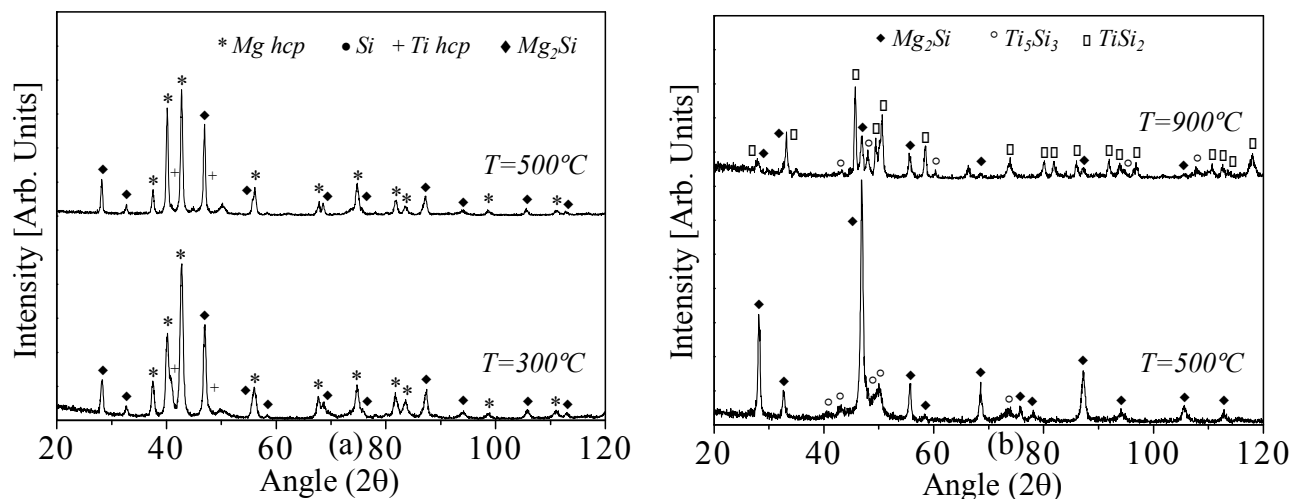


Fig. 2. Structural evolution of the (a)  $\text{Mg}_{88}\text{Ti}_5\text{Si}_7$  and (b)  $\text{Mg}_{60}\text{Ti}_{10}\text{Si}_{30}$  mixtures with temperature.

**Corrosion tests.** The various types of corrosion test were carried out, at least three times for each experimental condition to assess experimental reproducibility.

*Open circuit potential (OCP).* Immersion in electrolyte solution leads to an increase of the open circuit potential over a period of about 20 minutes and the formation of a black layer on the sample surface which can be attributed to the formation of oxides. Pitting corrosion then occurs, most visibly in NaCl solution, with the formation of further black products. It was not possible to see large differences between the different types of sample by visual inspection.

Examination of the surfaces of the samples of the  $\text{Mg}_{88}\text{Ti}_5\text{Si}_7$  alloy by scanning electron microscopy following corrosion showed the formation of pits (Fig. 3a). These pits were even detected (in small number) in the samples tested with the less aggressive sodium sulphate solution. These pits can be

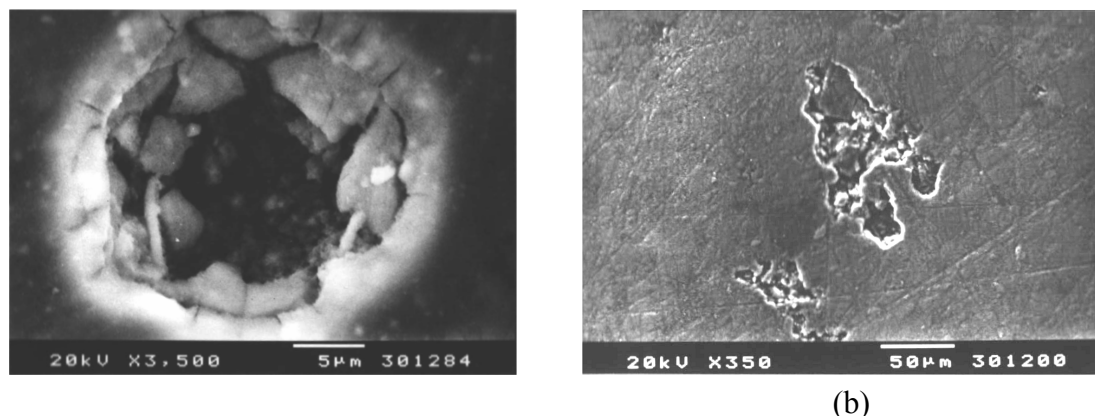


Fig. 3. SEM typical images of corroded (a)  $\text{Mg}_{88}\text{Ti}_5\text{Si}_7$  milled for 25 h without heat treatment and (b)  $\text{Mg}_{60}\text{Ti}_{10}\text{Si}_{30}$  after 900°C heat treatment.

attributed to corrosion of the magnesium metal phase, particularly at flaws in the surface. There is also some more uniform, less deep, corrosion, probably of  $\text{Mg}_2\text{Si}$ .

With respect to the  $\text{Mg}_{60}\text{Ti}_{10}\text{Si}_{30}$  alloy, the observed corrosion is less. In this alloy there is no magnesium metal, and the  $\text{Mg}_2\text{Si}$  phase slowly dissolves in localised areas, probably associated with defects in the alloy phase where the local potential is more positive, thus promoting anodic dissolution - see the example in Fig 3b. Electron probe microanalysis confirmed the formation of an oxide layer of titanium and magnesium oxides.

*Polarisation curves.* Analysis of the polarisation curves recorded after stabilisation of the open circuit potential leads to values of the corrosion potential and corrosion current. In sodium sulphate

solution the corrosion current was of the order of  $30 \mu\text{A cm}^{-2}$  and did not permit clear distinctions between the different milling times and heat treatments. However, in sodium chloride solution currents reached an order of magnitude higher and significant differences were seen between the different sintering conditions and heat treatments for the alloys, as shown in Fig.4.

The corrosion currents of the  $\text{Mg}_{60}\text{Ti}_{10}\text{Si}_{30}$  samples are significantly lower than of the samples of  $\text{Mg}_{88}\text{Ti}_5\text{Si}_7$ . Average values lower than  $50 \mu\text{A cm}^{-2}$  were obtained for the alloy with higher silicon content. The corrosion resistance of the  $\text{Mg}_{88}\text{Ti}_5\text{Si}_7$  alloy increases with milling time (formation of  $\text{Mg}_2\text{Si}$  intermetallic phase).

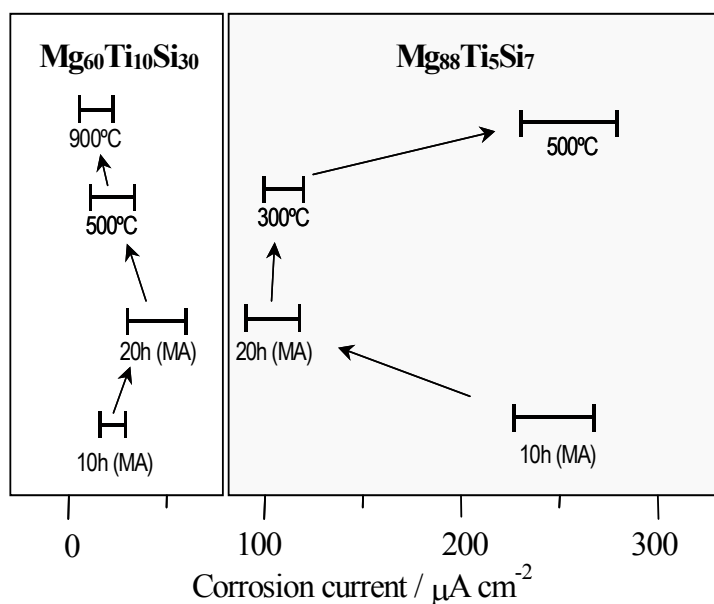


Fig.4. Corrosion current density in 0.01M NaCl solution of the  $\text{Mg}_{60}\text{Ti}_{10}\text{Si}_{30}$  and  $\text{Mg}_{88}\text{Ti}_5\text{Si}_7$  samples after different ball milling times and subsequent annealing.

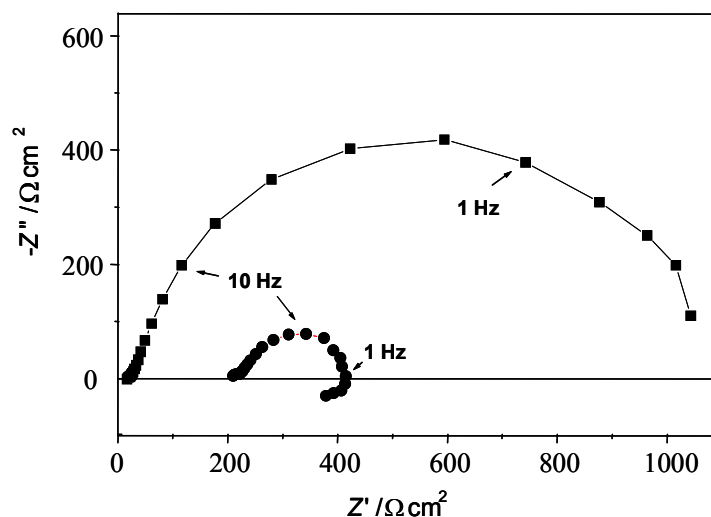


Fig.5. Complex plane impedance spectra of  $\text{Mg}_{88}\text{Ti}_5\text{Si}_7$  alloy (milling time 25 h, heat treatment  $300^\circ\text{C}$ ) in ■ 0.1 M  $\text{Na}_2\text{SO}_4$  and ● 0.01 M NaCl solution.

circuit analysis suggests that it is slower, in agreement with results from polarisation curves.

The corrosion resistance of this alloy decreases drastically for high annealing temperatures ( $500^\circ\text{C}$ ). This can be explained by the fact that this temperature is close to the melting point of Mg, the element which constitutes the matrix of this sample.

Concerning the  $\text{Mg}_{60}\text{Ti}_{10}\text{Si}_{30}$  alloy, the increase of milling time seems to slightly decrease its corrosion resistance. Annealing at temperatures of 500 and  $900^\circ\text{C}$  is beneficial for the corrosion resistance of this alloy. It is important to note that, as pointed out previously, phase transformations were detected during annealing of this sample. In fact, the appearance of  $\text{Ti}_5\text{Si}_3$  and  $\text{TiSi}_2$  during annealing at 500 and  $900^\circ\text{C}$ , respectively, might be responsible for this increase in corrosion resistance.

**Electrochemical impedance.** Complex plane impedance spectra of the  $\text{Mg}_{88}\text{Ti}_5\text{Si}_7$  alloy, as in Fig.5, all had a semicircular form at the frequencies tested, as observed for other magnesium alloys [4]. The larger semicircles obtained demonstrated that corrosion is less in sodium sulphate than in sodium chloride solution, even though the ionic strength is much higher. Regarding  $\text{Mg}_{60}\text{Ti}_{10}\text{Si}_{30}$ , the alloy surface was too unstable to record impedance spectra in sodium chloride solution, even at  $10^{-2}\text{M}$  concentrations.

In sodium sulphate solution, the corrosion process was less uniform and slower than at the other alloy, although equivalent

## Conclusions

The experimental results shows that the corrosion resistance of the  $\text{Mg}_{60}\text{Ti}_{10}\text{Si}_{30}$  alloy is higher than that of  $\text{Mg}_{88}\text{Ti}_5\text{Si}_7$ , which is explained in terms of chemical composition and changes in the alloy microstructure occurred during milling and subsequent heat treatment. The larger the quantity of intermetallics formed the higher the resistance to corrosion. For the  $\text{Mg}_{88}\text{Ti}_5\text{Si}_7$  alloy this property increases with milling time and decreases drastically for high annealing temperatures. Contrarily, the heat treatment is beneficial for the corrosion resistance of the sample rich in silicon ( $\text{Mg}_{60}\text{Ti}_{10}\text{Si}_{30}$  alloy).

## References

- [1] S.B. Dodd, S. Morris and M. Wardclose: *Synthesis of Lightweight Metals III*, pp. 117-184 (F.H. Froes, Ed. Warrendale; Minerals Metals & Materials Soc. 1999).
- [2] L. Dias, B. Trindade, C. Coelho and F.H. Froes: *Key Eng. Mat.* Vols. 230-232 (2002), p. 283.
- [3] G. Song, A. Atrens, D. St. John, X. Wu and J. Nairn: *Corros. Sci.* Vol. 39 (1997), p.1981.
- [4] G. Baril, C. Blanc and N. Pebère: *J. Electrochem. Soc.* Vol. 148 (2001), p. B489.